Polymer 50 (2009) 6009–6018

Contents lists available at ScienceDirect

Polymer

journal homepage: www.elsevier.com/locate/polymer

Synthesis and characterization of highly optical transparent and low dielectric constant fluorinated polyimides

Liming Tao, Haixia Yang*, Jingang Liu, Lin Fan, Shiyong Yang*

Laboratory of Advanced Polymer Materials, Institute of Chemistry, Chinese Academy of Sciences, Beijing 100190, China

ARTICLE INFO

Article history:
Received 9 June 2009
Received in revised form
12 September 2009
Accepted 11 October 2009
Available online 22 October 2009

Keywords:
Fluorinated polyimides
High transparency
Dielectric properties

ABSTRACT

Multitrifluoromethyl-substituted aromatic diamines, 1,1-bis[4-(4′- amino-2′-trifluoromethylphenoxy)-phenyl]-1-(3″-trifluoromethylphenyl)-2,2,2-trifluoroethane (12FDA) and 1,1-bis[4-(4′-amino-2′-trifluoromethylphenoxy)phenyl]-1-[3″,5″-bis (trifluoromethyl)phenyl]-2,2,2-trifluoroethane (15FDA) were synthesized, which were employed to react with various aromatic dianhydrides to yield a series of highly fluorinated polyimides. The fluorinated polyimides synthesized showed great solubility with inherent viscosities of 0.47–0.69 dL/g. The strong and tough polyimide films exhibited good thermal stability with the glass transition temperature (T_g) of 209–239 °C and outstanding mechanical properties with the tensile strengths of 88–111 MPa and tensile modulus of 2.65–3.17 GPa. Dielectric constants of as low as 2.49 and low moisture absorptions (0.17–0.66%) were measured. The fluorinated polyimide films (7–10 μm in thickness) also showed highly optical transparency with light transmittance at 450 nm of as high as 97.0% and cutoff wavelength of as low as 298 nm. The average refractive indices and birefringence of the fluorinated polyimide films were measured in the range of 1.5060–1.5622 and 0.0036–0.0095, respectively. PI-7 and PI-8 exhibited low light-absorption in the near-infrared region, especially at the optocommunication wavelength of 1310 nm and 1550 nm.

1. Introduction

As a kind of high performance polymer, aromatic polyimides are well known for their high thermal stability, excellent mechanical properties, outstanding dimensional stability and chemical resistance [1–5]. In recent years, aromatic polyimides with good combination of high optical transparency, low refractive index (low-*n*), low dielectric constant (low-*k*), high glass transition temperature as well as outstanding mechanical properties have been drawn intense attention for advanced microelectronic and optoelectronic applications [6–8]. In general, aromatic polyimides are difficult for both solution-casting and melt processing due to their poor solubility in organic solvents and high melting temperatures. Hence, aromatic polyimides with good processability are required for widespread applications in high-tech industries. Additionally, the standard aromatic polyimides showed yellow to brown in colors due to the intra- and inter-molecular charge transfer (CT) interactions between the alternating electron-donor (diamine) and electron-acceptor (dianhydride) moieties [9–11]. Therefore, considerable efforts have been made in recent years to develop highly optical transparent, low-*k* and low-*n* aromatic polyimides with good processability by using of polyisoimides as the polyimide precursor [12–14] or by introducing of flexible linkages, fluorinated substituents, unsymmetrical units or bulky pendent groups into the polymer backbones [15–32]. Among the above-mentioned strategies, introducing of fluorinated substituents such as hexafluoroisopropylidene linkages, perfluoroalkyl groups, pendent trifluoromethyl groups have been considered as one of the most promising methods. As well-known, the high electronegativity and low molar polarization of the fluorinated groups could endow aromatic polyimides with many attractive features, such as good organo-solubility, high optical transparency, low dielectric constant, as well as low water uptake [33–44]. However, the fluorinated groups attached in the chemical structures of aromatic diamine monomers could usually reduce the condensing reactivity of the diamine with aromatic dianhydride, resulting in aromatic polyimides with poor mechanical properties caused by the relatively low molecular weights. Hence, how to design and synthesize fluorinated aromatic diamines as the monomers of polyimides has still been a scientific and technological challenge.

In this study, novel multitrifluoromethyl-substituted aromatic diamines, 1,1-bis[4-(4′-amino-2′-trifluoromethylphenoxy)phenyl]-1-(3″-trifluoromethylphenyl)-2,2,2-trifluoroethane (12FDA) and 1,1-bis[4-(4′-amino-2′-trifluoromethylphenoxy)phenyl]-1-[3″,5″-

* Corresponding authors. Tel.: +86 10 62564819; fax: +86 10 62569562.
E-mail addresses: yanghx@iccas.ac.cn (H. Yang), shiyang@iccas.ac.cn (S. Yang).

0032-3861/$ – see front matter © 2009 Elsevier Ltd. All rights reserved.
doi:10.1016/j.polymer.2009.10.022

bis(trifluoromethyl)phenyl]-2,2,2-trifluoroethane (15FDA) were synthesized, which were then employed to react with different aromatic dianhydrides by a one-step thermal polycondensation procedure to yield a series of highly fluorinated aromatic polyimides. Effect of the polymer backbone structures on their solubility, thermal stability, mechanical properties, dielectric properties, refractive indices and birefringence, as well as optical transparency was systematically investigated.

2. Experimental

2.1. Materials

2-Chloro-5-nitrotrifluoromethylbenzene was prepared in this laboratory according to the literature [42]. 3′-trifluoromethyl-2,2,2-trifluoroacetophenone(6FK) [37] and 3′,5′-ditrifluoromethyl-2,2,2-trifluoroacetophenone (9FK) [38] were synthesized in this laboratory according to the previously reported method. 4,4′-Oxydiphthalic anhydride (ODPA, Shanghai Chemspec. Co.) was recrystallized from acetic anhydride prior to use. 4,4-(Hexafluoroisopropylidene)diphthalic anhydride (6FDA, Hoechst Celanese Corp.) was dried at 160 °C overnight prior to use. 3,3′,4,4′-Benzophenonetetracarboxylic dianhydride (BTDA, Acros) was recrystallized from acetic anhydride and dried in a vacuum oven at 160 °C for 10 h. 3,3′,4,4′-Biphenyltetracarboxylic dianhydride (BPDA, Ube Industries Ltd, Japan) was purchased and dried in a vacuum oven at 180 °C for 12 h prior to use. Trifluoromethanesulfonic acid (TFSA) was purchased from Shanghai Everthriving Co. and used without further purification. Phenol and anhydrous potassium carbonate were purchased from Beijing Chemical Reagents Co., China and used as received. Commercially available *N*-methyl-2-pyrrolidinone (NMP), *m*-cresol, and *N,N*-dimethylacetamide (DMAc) were purified by vacuum distillation over CaH_2 and stored over 4 Å molecular sieves prior to use. Other solvents were used as received.

2.2. Measurements

NMR spectra were performed on a Bruker Avance 400 Spectrometer operating at 400 MHz for ^{1}H NMR and 100 MHz for ^{13}C NMR, using DMSO–d_6 or $CDCl_3$ as the solvents. Fourier transform infrared (FT-IR) spectra were recorded on a Perkin–Elmer 782 Fourier transform spectrophotometer. Ultraviolet-visible (UV–vis) spectra were recorded on a Hitachi U3210 spectrophotometer at room temperature. Prior to testing, film samples were dried at 100 °C for 1 h to remove the absorbed moisture. Near-infrared spectra were measured by a Shimadzu UV-3100 UV/Vis/NIR spectrophotometer. Mass spectra were recorded on an AEI MS-50 mass spectrometer. The wide-angle X–ray diffraction (XRD) was conducted on a Rigaku D/max-2500 X–ray diffractometer with Cu/K-α1 radiation, operated at 40 kV and 200 mA. Differential Scanning Calorimetry (DSC), Thermogravimetric analysis (TGA) were recorded on a TA Q series thermal analysis system in nitrogen at a heating rate of 20 °C/min. Thermomechanical analysis (TMA) were recorded on a Perkin–Elmer 7 series thermal analysis system in nitrogen at a heating rate of 10 °C/min. Inherent viscosities were measured with an Ubbelohde viscometer with 0.5 g/dL NMP solution at 30 °C. The absolute viscosities (η_a) were measured using a Brookfield DV-II+ viscometer at 25 °C. The mechanical properties were measured on an Instron-3365 Tensile Apparatus with $80 \times 10 \times 0.05$ mm^3 specimens in agreement with GB 1447-83 at a drawing rate of 2.0 mm/min. The electrical insulation properties were measured on a ZC36 Precision Resistivity Meter. The surface and volume resistances were measured with film specimens with a diameter of 50 mm and a thickness of 50 μm. Samples were dried at 120 °C for 1 h to eliminate absorbed moisture prior to testing. Water uptakes were determined by weighing the changes of polyimide film ($3.0 \times 1.0 \times 0.005$ cm^3) before and after immersion in water at 25 °C for 24 h. Solubility was measured by mixing of dried polyimide resin (1.5 g) in the solvents (8.5 g) at room temperature (15% resin concentration), followed by stirring in nitrogen for 24 h. The refractive indices of the polyimide films formed on a 3-inch silicon wafer were measured at a wavelength of 1310 nm at room temperature with a Sairon Tech Model SPA–4000 prism coupler. The in-plane (n_{TE}) and out-of-plane (n_{TM}) refractive indices were determined by using linearly polarized laser light polarizations parallel (transverse electric, TE) and perpendicular (transverse magnetic, TM) to the film plane. The in-plane (n_{TE})/out-of-plane (n_{TM}) birefringence (Δn) was calculated as the difference between the n_{TE} and n_{TM}. The average refractive index (n_{AV}) was calculated by Eq. (1):

$$n_{AV} = \sqrt{(2n_{TE}^2 + n_{TM}^2)/3} \quad (1)$$

2.3. Monomer synthesis

2.3.1. 2-Trifluoromethyl-4-nitrophenyl phenyl ether (3FNPE)

A mixture of phenol (7.53 g, 80.0 mmol), 2-chloro-5-nitrotrifluoromethylbenzene (18.95 g, 84.0 mmol), anhydrous potassium carbonate (11.08 g, 80.0 mmol), and anhydrous DMAc (120 mL) was added to a three-necked, 250-mL, round-bottom flask fitted with a nitrogen inlet pipet, a thermometer, a condenser and a mechanical stirrer. The mixture was heated with stirring to 130–135 °C in nitrogen for 24 h. Then some of the solvent was removed by vacuum distillation. The mixture was then poured into an excess amount of ice-water. The precipitate was collected by filtration, washed several times with water, and dried in oven. The product was recrystallized from ethyl ethanol to give yellow crystals: 21.07 g [Yield: 93.0%; mp: 65.0–66.5 °C by DSC in N_2, 10 °C/min].

FT-IR (KBr pellets, cm^{-1}): 3099, 1628, 1592, 1537, 1486, 1436, 1354, 1286, 1162, 902. ^{1}H NMR (400 MHz, $CDCl_3$, δ, ppm): 8.60 (d; 1H, H_a), 8.31 (q; 1H, H_b), 7.49 (t; 2H, H_c), 7.33 (t; 1H, H_d), 7.13 (d; 2H, H_e), 6.95 (d; 1H, H_f). ^{13}C NMR (100 MHz, DMSO-d_6, δ, ppm): 160.8 (C^1), 154.4 (C^2), 142.1 (C^3), 131.2 (C^4), 130.5 (C^5), 126.7 (C^6), 123.8 (C^7), 122.6 (q, $^1J_{C-F} = 273.3$ Hz, C^8), 120.9 (C^9), 119.5 (q, $^2J_{C-F} = 32.3$ Hz, C^{10}), 118.5 (C^{11}). TOF–MS (electron ionization, *m*/*e*, percentage of relative intensity): 283(M^+, 100), 253 ($(M-30)^+$, 55). Elem. Anal. Calcd. for $C_{13}H_8F_3NO_3$: C, 55.13%; H, 2.85%; N, 4.95%. Found: C, 55.01%; H, 2.86%; N, 4.88%

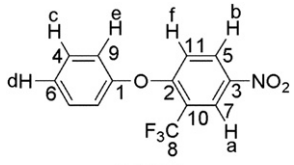

3FNPE

2.3.2. 1,1-Bis[4-(4′-nitro-2′-trifluoromethylphenoxy)phenyl]-1-(3″-trifluoromethyl phenyl)-2,2,2-trifluoroethane (12FDN)

A mixture of 6FK (24.2 g, 0.10 mol), 3FNPE (62.30 g, 0.22 mol) and anhydrous 1,2-dichloroethane (100 mL) was added to 250-mL round-bottom flask fitted with a dropping funnel, drying tube and magnetic stirrer. Trifluoromethanesulfonic acid (16.50 g, 0.11 mol) was added dropwise at room temperature. After completion of the addition, the mixture was stirred at room temperature for 48 h. The mixture was then poured into excess of distilled water. The precipitate was collected by filtration, washed with 5% of aqueous sodium bicarbonate solution, distilled water and methanol,

respectively. The precipitate obtained was dried in oven to give a yellow solid, which was then recrystallized from 2-methoxy-ethanol to give pale yellow powder: 55.3 g. [Yield: 70.0%; mp: 129.0–130.0 °C by DSC in N_2, 10 °C/min].

FT-IR (KBr pellets, cm^{-1}): 3099, 1628, 1592, 1537, 1486, 1436, 1354, 1329, 1286, 1162, 902, 678. ^1H NMR (400 MHz, DMSO-d_6, δ, ppm): 7.80 (d; 1H, H_c), 7.72 (t; 1H, H_b), 7.44 (d; 1H, H_a), 7.19 (s; 1H, H_d), 6.98 (m; 4H, H_e, H_g), 6.92 (d; 8H, H_h, H_i), 6.84 (d; 2H, H_f). ^{13}C NMR (100 MHz, DMSO-d_6, δ, ppm): 160.2 (C^1), 154.5 (C^2), 142.5 (C^3), 140.8 (C^4), 136.6 (C^5), 133.8 (C^6), 132.2 (C^7), 130.6 (q, $^2J_{C-F} = 32$ Hz, C^8), 130.0 (C^9), 129.6 (C^{10}), 129.2 (C^{11}), 124.2 (q, $^1J_{C-F} = 270$ Hz, C^{12}), 126.0 (C^{13}), 125.4 (C^{14}), 121.2 (q, $^1J_{C-F} = 271$ Hz, C^{15}), 122.1 (q, $^1J_{C-F} = 286$ Hz, C^{16}), 123.5 (C^{17}), 120.6 (C^{18}), 118.5 (C^{19}), 64.6 (q, $^2J_{C-F} = 20$ Hz, C^{20}). TOF–MS (electron ionization, *m*/*e*, percentage of relative intensity): 790 (M^+, 14), 721($(M-69)^+$, 100). Elem. Anal. Calcd. for $C_{35}H_{18}F_{12}N_2O_6$: C, 53.18%; H, 2.30%; N, 3.54%. Found: C, 53.14%; H, 2.34%; N, 3.50%.

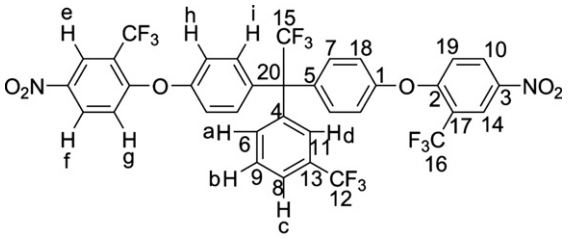

2.3.3. 1,1-Bis[4-(4′-amino-2′-trifluoromethylphenoxy)phenyl]-1-(3″-trifluoromethyl phenyl)-2,2,2-trifluoroethane (12FDA)

A slurry of the purified dinitro-compound 12FDN (23.72 g, 0.03 mol), 5% Pd/C (0.40 g) in ethanol (200 mL) was heated at 70–80 °C. Then hydrazine monohydrate (20.0 mL) was added dropwise within 30 min, and the mixture was heated to reflux for 8 h. The reaction solution was filtered hot to remove Pd/C, and the filtrate was then distilled to remove the solvent. The obtained mixture was poured into an excess amount of distilled water to give a precipitate. After collected and washed with water, the white solid powder was dried in vacuum to give 12FDA: 20.38 g [Yield: 93.0%].

FT-IR (KBr pellets, cm^{-1}): 3478, 3396, 3049, 1636, 1608, 1500, 1458, 1334, 1230, 1160, 1043, 865, 833, 678. ^1H NMR (400 MHz, DMSO-d_6, δ, ppm): 5.49 (s; 4H, $-NH_2$), 6.82 (q; 2H, H_i), 6.97–6.91 (m; 8H, H_f, H_g, H_h), 7.00 (d; 4H, H_e), 7.22 (s; 1H, H_d), 7.46 (d; 1H, H_c), 7.72 (t; 1H, H_b), 7.82 (d; 1H, H_a). ^{13}C NMR (100 MHz, DMSO-d_6, δ, ppm): 158.2 (C^1), 146.1 (C^2), 141.5 (C^3), 140.9 (C^4), 133.4 (C^5), 132.2 (C^6), 130.7 (C^7), 129.8 (C^8), 129.2 (q, $^2J_{C-F} = 31.5$ Hz, C^9), 127.5 (q, $^1J_{C-F} = 284.4$ Hz, C^{10}), 123.4 (q, $^1J_{C-F} = 270.9$ Hz, C^{11}), 125.2 (C^{12}), 125.0 (C^{13}), 123.8 (q, $^1J_{C-F} = 270.9$ Hz, C^{14}), 123.5 (C^{15}), 121.6 (q, $^2J_{C-F} = 29.9$ Hz, C^{16}), 118.5 (C^{17}), 116.3 (C^{18}), 110.7 (C^{19}), 63.3 (q, $^2J_{C-F} = 24$ Hz, C^{20}). TOF–MS (electron ionization, *m*/*e*, percentage of relative intensity): 730(M^+, 48), 661($(M-69)^+$, 100). Elem. Anal. Calcd. for $C_{35}H_{22}F_{12}N_2O_2$: C, 57.54%; H, 3.04%; N, 3.83%. Found: C, 57.52%; H, 3.05%; N, 3.79%.

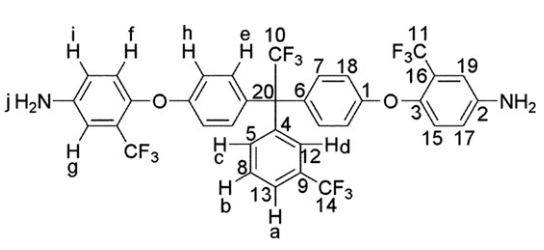

2.3.4. 1,1-Bis[4-(4′-nitro-2′-trifluoromethylphenoxy)phenyl]-1-[3″,5″-bis(trifluoro-methyl)phenyl]-2,2,2-trifluoroethane (15FDN)

A mixture of 9FK (31.0 g, 0.10 mol), 3FNPE (62.30 g, 0.22 mol), and anhydrous 1,2-dichloroethane (100 mL) was added to 250-mL of round-bottom flask fitted with a dropping funnel, drying tube, and magnetic stirrer. Trifluoromethanesulfonic acid (16.50 g, 0.11 mol) was added dropwise at room temperature. After completion of the addition, the mixture was stirred at room temperature for 48 h. The mixture was poured into an excess amount of distilled water. The precipitate was collected by filtration, washed with 5% of aqueous sodium bicarbonate solution, distilled water and methanol, respectively. The yellow solid product was dried in oven, then recrystallized from 2-methoxy-ethanol: 64.40 g [Yield: 75.0%; mp: 167.0–169.0 °C by DSC in N_2, 10 °C/min].

FT-IR (KBr pellets, cm^{-1}): 3099, 1626, 1600, 1530, 1489, 1360, 1285, 1157, 1051, 901, 682. ^1H NMR (400 MHz, DMSO-d_6, δ, ppm): 7.27 (m; 6H, H_c, H_g), 7.35 (d; 4H, H_d), 7.64 (s; 2H, H_b), 8.34 (s; 1H, H_a), 8.50 (d; 2H, H_f), 8.53 (s; 2H, H_e). ^{13}C NMR (100 MHz, DMSO-d_6, δ, ppm): 160.0 (C^1), 154.8 (C^2), 142.7 (C^3), 142.6 (C^4), 135.7 (C^5), 132.2 (C^6), 131.7 (q, $^2J_{C-F} = 33$ Hz, C^{13}), 130.0 (C^7), 129.7 (C^8), 127.5 (q, $^1J_{C-F} = 284$ Hz, C^{14}), 123.3 (q, $^1J_{C-F} = 271$ Hz, C^{15}), 122.5 (q, $^1J_{C-F} = 271$ Hz, C^{16}), 123.5 (C^9), 122.9 (C^{10}), 120.7 (C^{11}), 120.6 (q, $^2J_{C-F} = 32$ Hz, C^{17}), 118.7 (C^{12}), 64.6 (q, $^2J_{C-F} = 20$ Hz, C^{18}). TOF–MS (electron ionization, *m*/*e*, percentage of relative intensity): 858(M^+, 22), 789($(M-69)^+$, 100). Elem. Anal. Calcd. for $C_{36}H_{17}F_{15}N_2O_6$: C, 50.36%; H, 2.00%; N, 3.26%. Found: C, 50.37%; H, 2.03%; N, 3.22%.

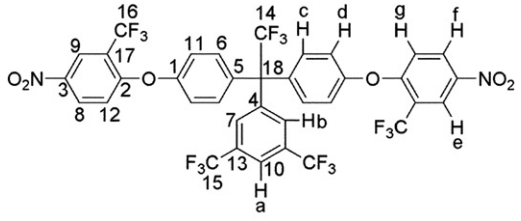

2.3.5. 1,1-Bis[4-(4′-amino-2′-trifluoromethylphenoxy)phenyl]-1-[3″,5″-bis(trifluoro-methyl)phenyl]-2,2,2-trifluoroethane (15FDA)

A suspension solution of the purified dinitro-compound 15FDN (25.76 g, 0.03 mol), 5% Pd/C (0.40 g) in ethanol (200 mL) was heated at 70–80 °C. Then hydrazine monohydrate (20.0 mL) was added dropwise within 30 min. The mixture was heated at reflux temperature for about 8 h. The reaction solution was filtered hot to remove Pd/C, and the filtrate was then distilled to remove the solvent. The obtained mixture was poured into an excess amount of water to give white precipitate, which was collected and washed with water, then dried in vacuum at room temperature to give the product 15FDA: 22.28 g [Yield: 93.0%].

FT-IR (KBr pellets, cm^{-1}): 3487, 3396, 3054, 1636, 1608, 1500, 1458, 1340, 1285, 1234, 1143, 1043, 865, 833, 678. ^1H NMR (400 MHz, DMSO-d_6, δ, ppm): 5.53 (s; 4H, $-NH_2$), 6.86 (q; 2H, H_g), 6.94–6.99 (m; 8H, H_d, H_e, H_f), 7.03 (d; 4H, H_c), 7.55 (s; 2H, H_b), 8.27 (s; 1H, H_a). ^{13}C NMR (100 MHz, DMSO-d_6, δ, ppm): 159.1 (C^1), 146.8 (C^2), 143.2 (C^3), 141.8 (C^4), 131.9 (C^5), 131.3 (C^6), 131.1 (q, $^2J_{C-F} = 30$ Hz, C^7), 129.9 (C^8), 127.8 (q, $^1J_{C-F} = 284.4$ Hz, C^9), 124.0 (q, $^1J_{C-F} = 270.8$ Hz, C^{10}), 124.2 (C^{11}), 123.4 (q, $^1J_{C-F} = 271.2$ Hz, C^{12}), 123.3 (C^{13}), 122.3 (q, $^2J_{C-F} = 30$ Hz, C^{14}), 119.0 (C^{15}), 117.0 (C^{16}), 111.3 (C^{17}), 64.0 (q, $^2J_{C-F} = 24$ Hz, C^{18}). TOF–MS (electron ionization, *m*/*e*, percentage of relative intensity): 798(M^+, 62), 729($(M-69)^+$, 100). Elem. Anal. Calcd. for $C_{36}H_{21}F_{15}N_2O_2$: C, 54.15%; H, 2.65%; N, 3.51%. Found: C, 54.10%; H, 2.67%; N, 3.50% (Scheme 1, Fig. 1).

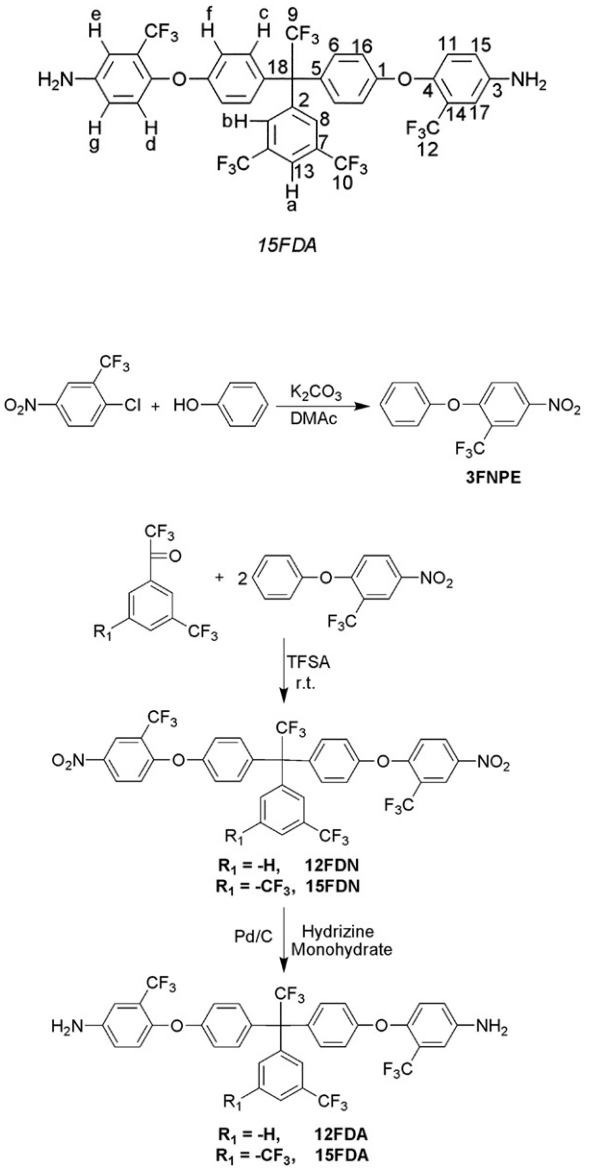

Scheme 1. Synthesis of the fluorinated diamine monomers.

2.4. Fluorinated polyimide synthesis

A series of polyimides were synthesized by polycondensation of 12FDA or 15FDA with various aromatic dianhydrides including BPDA, BTDA, ODPA and 6FDA, respectively. The synthesized polyimides were abbreviated as PI-1 to PI-8, successively, as shown in Scheme 2.

In a typical experiment, PI-3 derived from 12FDA and ODPA was synthesized by the following procedure. To a solution of 12FDA (2.1916 g, 3.00 mmol) in *m*-cresol (13.0 mL) placed in a 100-mL three-necked flask fitted with a mechanical stirrer, a nitrogen inlet, and a Dean-Stark trap, ODPA (0.9306 g, 3.00 mmol) was added in three portions. After the solution was stirred in nitrogen for 4 h, toluene (15.0 mL) was added. The reaction mixture was heated up to 180 °C and maintained for 12 h. During the polycondensation reaction, the toluene-water azeotrope was distilled out of the solution. After cooled down to room temperature, the homogeneous solution was slowly poured into excess of ethanol to give silky solid resin, which was collected, washed thoroughly with ethanol, and dried at 100 °C in vacuum for 8 h to give PI-3 resin with pale-yellow in color. The product yield was 95.0%.

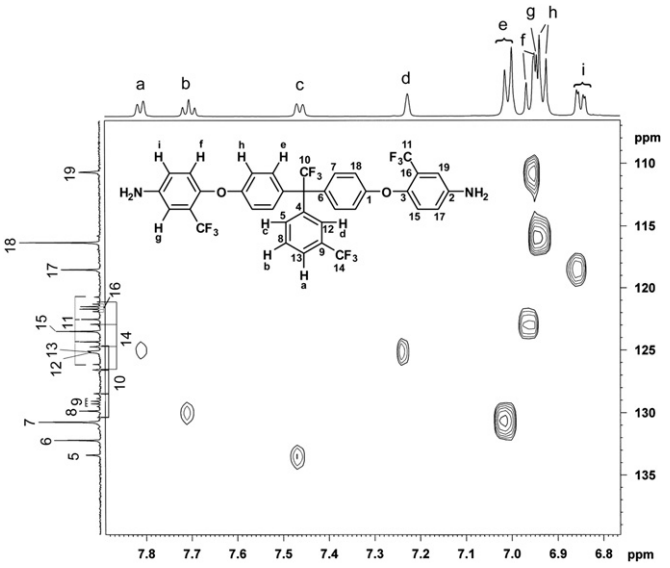

Fig. 1. HSQC spectrum of the fluorinated aromatic diamine (12FDA).

Other polyimides were synthesized in the same procedure as described above, except ODPA and 12FDA were replaced by the other aromatic diamine and aromatic dianhydrides as shown in Scheme 2 (Figs. 2 and 3, Table 1).

2.5. Polyimide film preparation

In a 100-mL three-necked round-bottomed flask, dried PI resin (6.0 g) was dissolved in anhydrous DMAc (24.0 g). The mixture was stirred at room temperature for 24 h to afford a viscous and homogeneous polyimide solution with a solid content of 20 wt%. The polyimide solution was filtered via a 0.2-mm Teflon syringe in order to remove any solid impurities. The filtrated solution was cast onto a glass plate which was then thermally baked at 80 °C for 4 h, 120 °C for 1 h, 150 °C for 1 h, and 220 °C for 1 h, successively. The free-standing polyimide film was stripped from the glass substrate by immersion in water followed by drying in an oven at 100 °C.

3. Results and discussion

3.1. Synthesis and characterization of aromatic diamine monomers

The fluorinated aromatic diamine monomers were prepared by the reaction sequence as shown in Scheme 1. 2-Trifluoromethyl-4-nitrophenyl phenyl ether (3FNPE), an intermediate mononitro-compound, was first synthesized by the chloro-displacement reaction of 2-chloro-5-nitrotrifluoromethylbenzene with phenol in the presence of potassium carbonate in DMAc. Then, dinitro-compounds (12FDN and 15FDN) were prepared by the couple reaction of the corresponding fluorinated aromatic ketones (6FK and 9FK) with 3FNPE in 1, 2-dichloroethane catalyzed by trifluoromethanesulfonic acid (TFSA) with high yields (70% for 12FDN and 75% for 15FDN, respectively). Finally, the aromatic diamine monomers, 1,1-bis[4-(4′-amino-2′-trifluoromethyl phenoxy)phenyl]-1-(3″-trifluoromethylphenyl)-2,2,2-trifluoroethane (12FDA) and 1,1-bis[4-(4′-amino-2′-trifluoromethylphenoxy)phenyl]-1-[3″,5″-bis(trifluoromethyl)phenyl]-2,2,2-trifluoroethane (15FDA), were obtained by the catalytic reduction of intermediate dinitro-compounds (12FDN and 15FDN) with hydrazine monohydrate and Pd/C catalyst in refluxing ethanol in high yields.

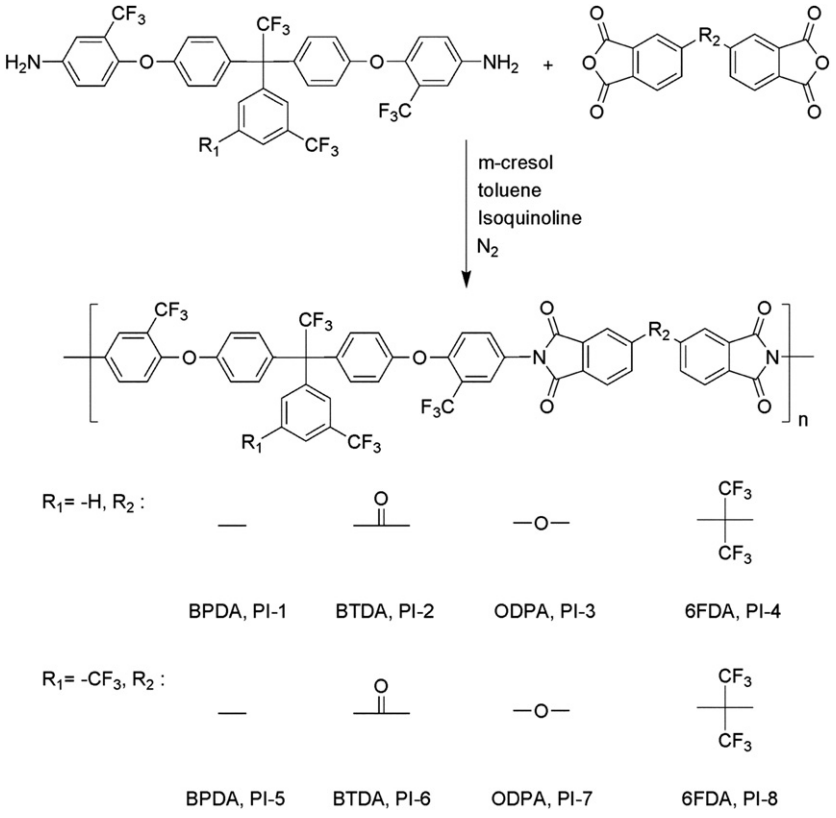

Scheme 2. Synthesis of the fluorinated polyimides.

The chemical structures of the synthesized aromatic diamines (12FDA and 15FDA) were confirmed by ^{1}H NMR, ^{13}C NMR, FT-IR, elemental analysis, MS spectrometry and two-dimensional COSY experiments. In the FT-IR spectra of dinitro-compounds and the corresponding diamine monomers, the absorption bands at 1580 and 1367 cm^{-1} assigned to the asymmetric and symmetric stretching vibrations of the nitro group (–NO_2) in 12FDN and 15FDN disappeared in the spectra of aromatic diamines (12FDA and 15FDA), whereas the characteristic absorptions of N–H stretching vibrations at 3403 cm^{-1} and 3480 cm^{-1} were observed in the aromatic diamine spectra, demonstrating that the nitro groups in dinitro-compounds were converted into the amine groups in aromatic diamines. Meanwhile, the absorption at 1145 cm^{-1} assigned to the C–F stretching vibration was also observed.

Fig. 1 shows a representative HSQC spectrum of the aromatic diamine (12FDA) in DMSO-d_6. The chemical shift of the protons in amino group was measured at 5.50 ppm in ^{1}H NMR (s, 4H, –NH_2). All of other protons could be clearly assigned as expected. In the ^{13}C NMR spectrum of 12FDA, carbon atoms resonated in the region of 110.7–158.2 ppm. C^{10} and C^{9} showed clear quartet absorptions at 124.7–130.7 and 128.8–129.5 ppm, respectively, due to the $^{1}J_{C-F}$ and

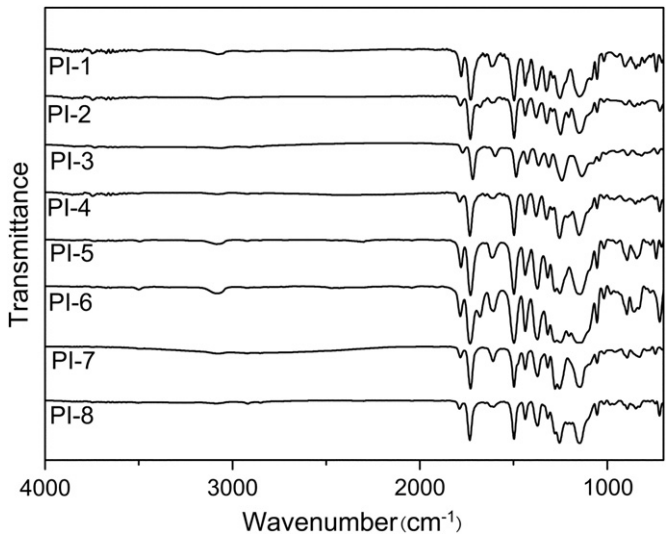

Fig. 2. FT-IR spectra of the fluorinated polyimides.

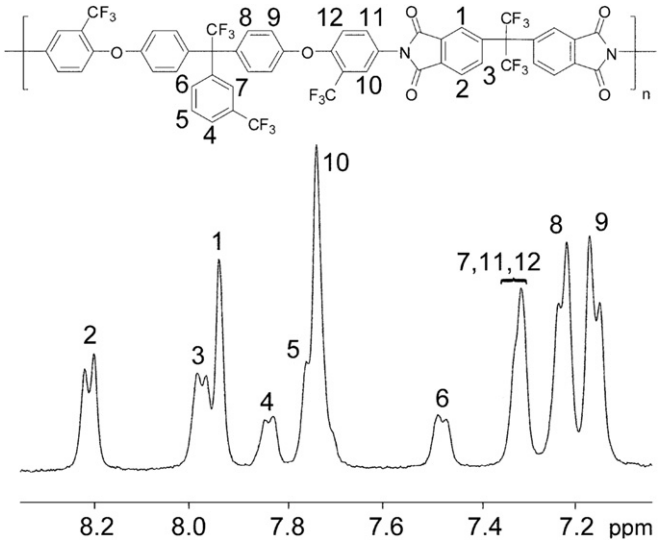

Fig. 3. ^{1}H NMR spectra of the fluorinated polyimide (PI-4) in DMSO-d_6 (400 MHz).

Table 1
Physical properties and elemental analysis of the fluorinated polyimides.

Code	Yield (%)	η_{inh} (dL/g)[a]	Formula (formula weight)	Elemental analysis (%)[b]			
					C	H	N
PI-1	98	0.54	$(C_{51}H_{24}F_{12}N_2O_6)_n$ [$(988.73)_n$]	Calcd	61.95	2.83	2.45
				Found	60.56	3.01	2.56
PI-2	94	0.62	$(C_{52}H_{24}F_{12}N_2O_7)_n$ [$(1016.74)_n$]	Calcd	61.43	2.76	2.38
				Found	59.60	2.89	2.64
PI-3	95	0.58	$(C_{51}H_{24}F_{12}N_2O_7)_n$ [$(1004.73)_n$]	Calcd	60.97	2.79	2.41
				Found	59.58	2.93	2.65
PI-4	95	0.49	$(C_{54}H_{24}F_{18}N_2O_6)_n$ [$(1138.75)_n$]	Calcd	56.96	2.46	2.12
				Found	56.71	2.65	2.34
PI-5	97	0.68	$(C_{52}H_{23}F_{15}N_2O_6)_n$ [$(1056.72)_n$]	Calcd	59.10	2.65	2.19
				Found	58.84	2.81	2.29
PI-6	93	0.58	$(C_{53}H_{23}F_{15}N_2O_7)_n$ [$(1084.73)_n$]	Calcd	58.68	2.14	2.58
				Found	58.45	2.79	2.26
PI-7	95	0.69	$(C_{52}H_{23}F_{15}N_2O_7)_n$ [$(1072.72)_n$]	Calcd	58.22	2.61	2.16
				Found	57.84	2.92	2.20
PI-8	95	0.47	$(C_{55}H_{23}F_{21}N_2O_6)_n$ [$(1206.75)_n$]	Calcd	54.74	2.32	1.92
				Found	54.23	2.46	1.93

[a] Measured in NMP at a concentration of 0.5 g/dL at 30 °C.
[b] All the samples were thermally baked at 200 °C for 3 h prior to test.

$^2J_{C-F}$ coupling of the carbon atoms with fluorine atoms in the diamine molecule. The coupling effect of carbon atom and fluorine atom were decreased with increasing of the distance between carbon atom and fluorine atom. For instance, C^{14} showed a stronger C–F coupling effect than C^9. The detail assignment of the protons and carbons was assisted by the two-dimensional COSY spectra as shown in Fig. 1, which is in well accordance with the proposed molecular structures. In addition, the elemental analysis values were also in good agreement with the calculated ones.

3.2. Synthesis of the fluorinated polyimides

In general, aromatic polyimide is synthesized from the condensation of aromatic diamine and aromatic dianhydride by either a two-step condensation polymerization method, i.e. the formation of poly(amic acid) (PAA) followed by a thermal or chemical imidization to give polyimide, or a one-step thermal polycondensation in solution at elevated temperature. In the present study, the fluorinated polyimides were prepared via the one-step thermal polycondensation as shown in Scheme 2. The thermal polycondensations were processed smoothly at temperature of 180 °C, and homogeneous, viscous polyimide solutions were produced, implying that the polycondensation reactivity of the aromatic diamine monomers was appropriate to the selected aromatic dianhydrides. It was seemed that the electron density of amino group in the aromatic diamines (12FDA and 15FDA) was not obviously reduced by the strong electron-withdrawing effect of the trifluoromethyl groups. Aromatic polyimides with reasonable high molecular weights could be obtained if the thermal polycondensation could be processed by sufficient time. In that case, fibrous polyimide resins with pale-yellow in color were obtained by pouring the polymer solution slowly into excess of ethanol.

Table 1 summarizes the physical features of the fluorinated polyimides, in which it can be seen that all of the polyimides were prepared in high yields (93–98%) and showed the inherent viscosities in the ranged of 0.47–0.69 dL/g, implying that the polymers have the reasonable high molecular weights. The elemental analysis data of the fluorinated polyimides were in good accordance with the calculated ones.

Fig. 2 depicts FT-IR spectra of the fluorinated polyimides, in which the characteristic imide group absorptions at 1780–1785 cm^{-1} assigned to the asymmetrical carbonyl stretching vibrations, and those at 1730 cm^{-1} assigned to the symmetrical carbonyl stretching vibrations, as well as that at 1371 cm^{-1} due to the C–N stretching vibrations were all observed. As expected, C–F multiple stretching absorptions were also measured at 1250 and 1145 cm^{-1}, respectively. The lack of amide and carboxyl absorptions indicated that the polymers were fully imidized from the intermediate poly(amic acid). The characteristic N–H stretching vibrations at around 3400 cm^{-1} were seldom observed in FT-IR spectra, implying that the multiple CF_3-substituted aromatic diamines showed appreciate polycondensation activity to the aromatic dianhydrides to yield aromatic polyimides. Fig. 3 shows a representative ^1H NMR spectrum of the fluorinated aromatic polyimide (PI-4) in DMSO-d_6, in which it can be seen that all of the protons could be well assigned to the expected polyimide structure.

3.3. Solubility and morphology of the fluorinated polyimides

The solubility of the fluorinated polyimides in different organic solvents was measured (Table 2). All of the polyimides could be

Table 2
Solubility of the fluorinated polyimides.

Code	Solvents[a]								
	NMP	DMAc	DMF	γ-Butyrolactone	$CHCl_3$	THF	Acetone	Toluene	Methanol
PI-1	++	++	++	+	++	++	++	+	−
PI-2	++	++	++	++	++	++	++	+	−
PI-3	++	++	++	++	++	++	++	+	−
PI-4	++	++	++	++	++	++	++	++	−
PI-5	++	++	++	++	++	++	++	+	−
PI-6	++	++	++	++	++	++	++	+	−
PI-7	++	++	++	++	++	++	++	++	−
PI-8	++	++	++	++	++	++	++	++	−

[a] ++: soluble at room temperature; +: soluble on heating; −: insoluble even on heating.

easily dissolved both in the strong polar solvents such as NMP, DMAc, DMF and in low boiling point solvents such as $CHCl_3$, THF, and acetone at room temperature. It was also found that the solubility of the fluorinated polyimides depended, to some extent, on the polymer backbone structures. For instance, PI-8 (6FDA–15FDA) showed the best solubility, which could even be easily dissolved in toluene. The outstanding solubility might be attributed to the high loadings of the trifluoromethyl groups in polymer backbones, which resulted in the reducing of the inter-chain interaction due to the non-coplanar structures and bulky substitutive effect.

Furthermore, the polyimide solubility was tested quantitatively. Fig. 4 compares the plots of absolute viscosities *vs* polyimide solid resin concentrations (PI-3) in different solvents including NMP, THF, and chloroform. It can be seen that the absolute viscosity would be increased dramatically when the resin concentration reached a critical point. The critical points differed from the solvents employed, i.e. 20 wt% for $CHCl_3$, 30 wt% for NMP and THF, respectively. For instance, the maximum polyimide concentration in NMP could be reached as high as 40 wt% with the solution viscosity of 4×10^4 mPa s, compared with 35% in THF with the solution viscosity of 1.6×10^4 mPa s and 25% in chloroform with the solution viscosity of 3.4×10^4 mPa s, respectively. If the polyimide solid concentration was increased higher than the critical point, the solution become unstable, and gelation would occur during the storing

Fig. 5 shows the wide-angle X–ray diffraction (XRD) patterns of the fluorinated polyimides, in which it can be seen that all of the synthesized polyimides are completely amorphous in morphologic structure. The polymer backbones with multiple trifluoromethyl groups and bulky aromatic side moieties would increase the disorder of the polymer chains, resulting in decreasing of the chain to chain interactions and reducing of chain packaging efficiency to hinder the polymer crystallization.

3.4. Thermal properties of the fluorinated polyimides

The glass transition temperatures of the polyimides were measured by DSC and DMA. In the DSC curves of the fluorinated polyimides, there is no melting endothermic behavior was observed except the glass transition temperatures (T_gs). The T_g values were measured in the range of 209–239 °C, of which PI-5(BPDA–15FDA) has the highest T_g (239 °C), 9 °C higher than PI-1 (BPDA–12FDA, 230 °C). In general, the 15FDA-based polyimides

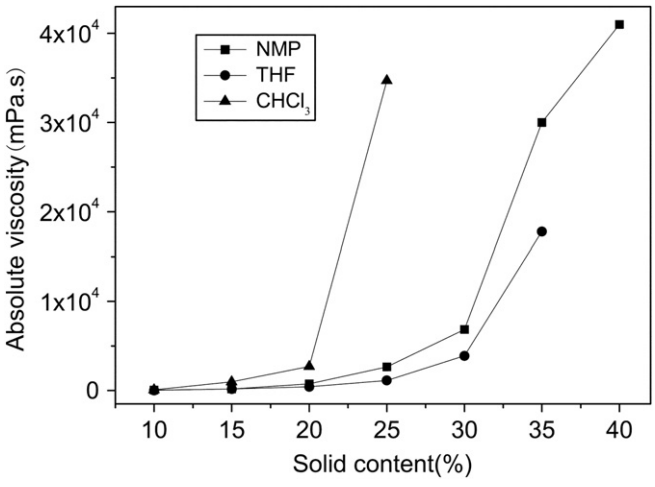

Fig. 4. Plot of absolute viscosity *vs* solid resin concentration (PI-3) in different solvents at 25 °C.

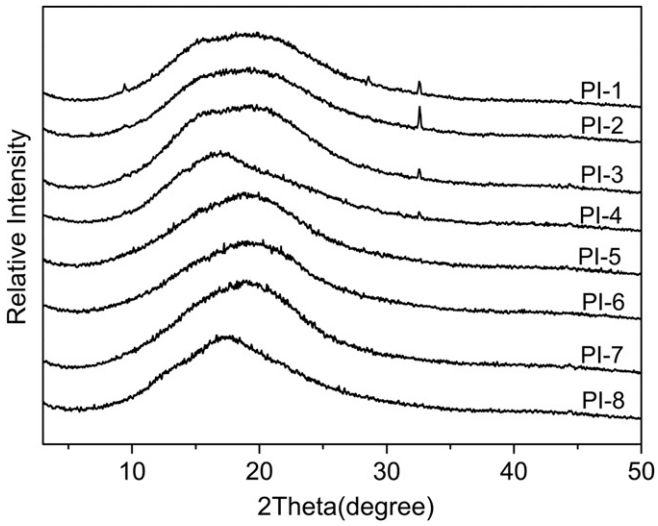

Fig. 5. XRD patterns of the fluorinated polyimides.

showed T_g values of 6–9 °C higher than the 12FDA-based ones, implying that the 15FDA-based polyimide backbones were more rigid than the 12FDA-based ones, probably due to the 3,5-ditrifluoromethyl-substituted phenyl group in polyimides (PI-5, 6, 7 or 8) was more steric hindrance than 3-trifluoromethyl-substituted phenyl group in polyimides (PI-1, 2, 3 or 4). In comparison, PI-3 (ODPA–12FDA) showed the lowest T_g value due to the presence of the flexible ether linkage and PI-5 (BPDA–15FDA) exhibited the highest T_g probably due to the rigid biphenyl unit in the polymer backbone.

Also the T_gs of the fluorinated polyimides were measured by DMA and the data were summarized in Table 3. The T_g values were measured in the range of 218–241 °C, of which PI-5(BPDA–15FDA) has the highest T_g (241 °C) and PI-3(ODPA–12FDA) has the lowest data (218 °C). The tendency is in well accordance with the results obtained by DSC. Generally, all of the polyimides except PI-8 showed higher T_g values measured by DMA than by DSC. As mentioned earlier, the polyimides with rigid units such as biphenyl linkages in polymer backbone have higher T_gs than those with flexible ether linkage (Table 3).

Fig. 6 compares the thermal stability of the fluorinated polyimides evaluated by TGA in nitrogen. No weight loss was detected until the temperature was scanned up to 450 °C. When the temperature was scanned up over 450 °C, all of the fluorinated polyimides showed more rapid thermal decomposition. The thermal decomposition temperatures (T_d) were measure in the range of 509–541 °C. The 5% (T_5) and 10% (T_{10}) of original weight

Table 3
Thermal properties of the fluorinated polyimides.

Code	T_g (°C)		T_d[a] (°C)	T_5[a] (°C)	T_{10}[a] (°C)	R_w[b] (%)	CTE[c] (ppm/°C)
	DSC	DMA					
PI-1	229.7	234.5	515.4	508.8	529.4	49.02	55.49
PI-2	219.0	238.2	510.8	511.3	533.3	57.78	48.85
PI-3	209.4	218.5	509.4	513.9	534.8	56.59	58.34
PI-4	227.5	238.1	508.9	509.8	528.6	54.24	55.94
PI-5	238.7	241.6	541.3	506.7	530.5	49.91	62.09
PI-6	226.8	238.6	539.3	510.9	533.6	49.68	58.20
PI-7	216.0	223.1	530.7	507.8	529.0	54.20	61.16
PI-8	234.2	231.0	516.1	504.3	521.8	43.11	61.77

[a] T_d, Onset decomposition temperature; T_5 and T_{10}, temperatures at 5% and 10% of original weight loss, respectively.
[b] Residual weight retention at 700 °C.
[c] The in-plane coefficients of thermal expansion at 50–200 °C.

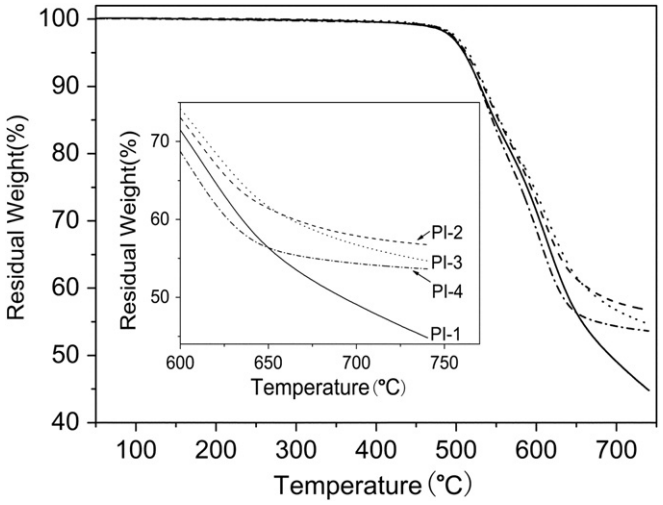

Fig. 6. TGA thermograms of the fluorinated polyimides.

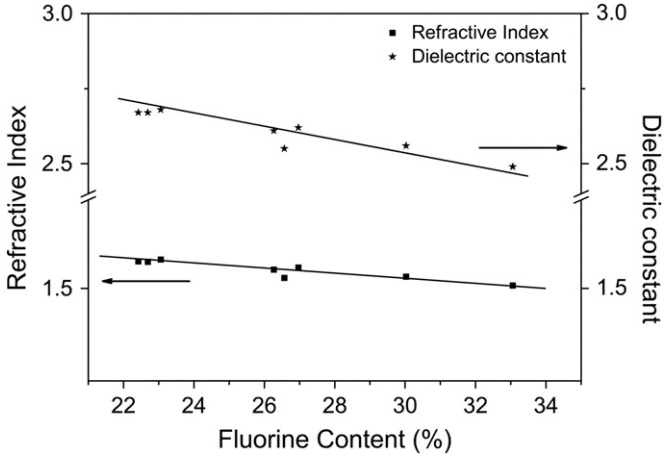

Fig. 7. Plots of refractive indices and dielectric constants *vs* fluorine loadings of the fluorinated polyimides at 1310 nm.

loss temperature were in the range of 504–514 °C and 522–535 °C in nitrogen, respectively (Table 3), and the char yields at 700 °C were all over 43% in nitrogen. The experimental results indicated that the fluorinated polyimides possessed great thermal stability to withstand the harsh environments of many high-tech applications such as microelectronic manufacturing and packaging industry. The in-plane coefficients of thermal expansion (CTE) for the fluorinated polyimides evaluated by TMA were in the range of 48.9–62.1 ppm/°C at the temperature of 50–200 °C.

3.5. Mechanical and electrical properties of the fluorinated polyimide films

All of the fluorinated polyimides could be cast into free-standing polyimide films with good mechanical properties including ultimate tensile strength of 88–111 MPa, an elongation at break of 5.4%–7.4%, and tensile modulus of 2.65–3.17 GPa, respectively (Table 4, Fig. 7).

The electrical insulating properties of the fluorinated polyimide films were shown in Table 4. The polyimide films showed good electrical insulating properties with surface resistance of 2.1–7.9 $\times 10^{14}$ Ω and volume resistance of 1.0–8.2 $\times 10^{15}$ Ω cm, respectively. The dielectric constants of the fluorinated polyimides were calculated from the refractive index n_{AV} according to Maxwell's equation: $\varepsilon = 1.10\, n_{AV}^2$, where an additional contribution of approximately 10% from the infrared absorption was included [45]. The dielectric constants were determined in the range of 2.49–2.68 (Table 4), which were not only much lower than the non-fluorinated polyimide such as PMDA–ODA (3.16) [46], but also lower than some of the fluorinated polyimides such as that derived from TFDAM and dianhydrides (2.73–2.82) [43] and that derived from 4FMA and dianhydrides (2.60–2.83) [44]. Fig. 7 shows the dependence of the dielectric constants on the fluorine loading in polyimide backbone. It can be seen that the dielectric constants were decreased gradually with increasing of the fluorine loadings. For instance, PI-8 (33.06% F) exhibited the lowest dielectric constant (2.49), compared with PI-1(23.06% F, $\varepsilon = 2.68$). The high electrical insulating and low dielectric constants of the fluorinated polyimides are mainly attributed to the high fluorine loadings in the polyimide backbones. The strong electronegativity of fluorine atoms would result in very low C–F polarizability, and the trifluoromethyl groups, combined with the high free volumes of side phenyl substituents, could endow the polyimides with low dielectric constants and high electrical insulating properties. Meanwhile, the phenylene ether units which could induce the dilution effect of the polar imide ring have also contributed to the reducing in the dielectric constants [24].

Table 4
Mechanical, electrical insulating and dielectric properties of the fluorinated polyimides.

Code	TS[a] (MPa)	EB[a] (%)	TM[a] (GPa)	$R_v \times 10^{-15}$ (Ω cm)[b]	$R_s \times 10^{-14}$ (Ω)[c]	ε[d]	Water uptake (%)
PI-1	91	6.1	2.78	8.2	4.3	2.68	0.42
PI-2	93	7.4	2.69	5.0	4.0	2.67	0.66
PI-3	96	7.4	2.65	1.5	5.5	2.67	0.50
PI-4	89	5.4	2.84	3.7	4.6	2.56	0.32
PI-5	94	5.9	2.87	6.7	4.0	2.62	0.21
PI-6	97	6.2	2.74	5.7	2.1	2.61	0.52
PI-7	111	5.7	3.17	1.0	7.9	2.55	0.35
PI-8	88	5.5	2.90	5.5	6.0	2.49	0.17

[a] TS: tensile strength; EB: elongation at break; TM: tensile modulus.
[b] Volume resistance.
[c] Surface resistance.
[d] Dielectric constant calculated from the equation: $\varepsilon = 1.10\, n_{AV}^2$.

The fluorinated polyimide films also exhibited very low water uptakes in the range of 0.17–0.66%, of which PI-8 showed the lowest water uptake (0.17%) compared with PI-1(0.66%). Clearly, the low water uptakes of the fluorinated polyimides were attributed to the high hydrophobicity derived from the presence of multiple trifluoromethyl groups in the polymer backbones.

3.6. Optical transparent properties of the fluorinated polyimide films

Fig. 8 shows the UV–vis spectra of the polyimide films. The polymer films (7–10 μm in thickness) are colorless and transparent with cutoff wavelength of as low as 298 nm and light transmittance of as high as 97.0% at 450 nm, respectively. It can be seen that the cutoff wavelength values showed decreasing tendency with the increasing of fluorine loading in the fluorinated polyimides. The minimum cutoff wavelength was detected at 298 nm for PI-4 and PI-8 with fluorine loading of >30 wt%. On the other hand, the light transmittance value at 450 nm was increased when the fluorine loading increased. For instance, PI-4 exhibited the highest light transparency at 450 nm (97.0%) and lowest cutoff wavelength (298 nm). Obviously, the optical property of PI-4 (6FDA–12FDA, 30.03% F) is better than the fluorinated polyimides reported in literatures. For instance, PI(9FDA–6FAPB, 29% F) [39] showed

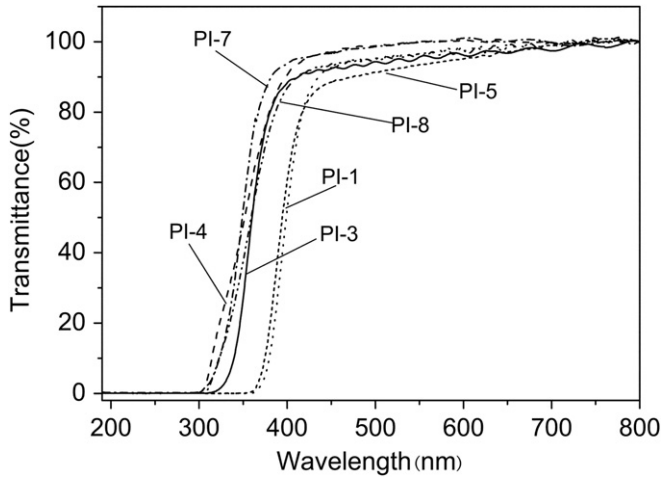

Fig. 8. UV–vis spectra of the fluorinated polyimides (film samples, 7–10 μm in thickness).

a cutoff wavelength of 330 nm and a transmittance of 83% at 450 nm; PI (6FDA–9FMA, 30.2% F) [40] showed a cutoff wavelength of 303 nm and a transmittance of 75.5% at 450 nm; PI(6FDA–4FMA, 25.2% F) [44] showed a cutoff wavelength of 318 nm and 82% of transmittance at 450 nm. This could be interpreted by the high fluorine loadings (>30 wt%) in the polymer backbones, which resulted in the reduction of the intermolecular charge-transfer complex (CTC) between alternating electron-donor (diamine) and electron-acceptor (dianhydride) moieties. The secondary effect of the fluorinated groups (trifluoromethyl) on the film transparency is the weakened intermolecular cohesive force due to the lower polarizability of the C–F bond, which would also resulted in the improvements in polyimide solubility in organic solvents [34]. Furthermore, the UV–vis spectra of the synthesized polyimide films with different thickness were compared as shown in Fig. 9. Obviously, the light transmittance at 450 nm decreased with increasing of the film thickness. However, the decreases in light transmittance depend upon, to some extent, the polyimide backbones. It can be seen that the ODPA-based polyimide showed better optical transparency than other dianhydride-based ones. For instance, PI-3(ODPA–12FDA) film exhibited as high as 80% of light transmittance at 450 nm even if the film thickness was 100 μm, compared with BPDA-based one (70%), BTDA or 6FDA-based one

Table 5
Refractive indices and birefringence of the fluorinated polyimide films

Code	d (μm) [a]	F (%)[b]	n_{TE}[c]	n_{TM}[d]	n_{AV}[e]	Δn[f]
PI-1	15.41	23.06	1.5641	1.5585	1.5622	0.0056
PI-2	14.86	22.42	1.5600	1.5553	1.5584	0.0047
PI-3	11.39	22.69	1.5588	1.5544	1.5573	0.0044
PI-4	12.02	30.03	1.5264	1.5228	1.5252	0.0036
PI-5	10.68	26.97	1.5458	1.5426	1.5447	0.0032
PI-6	14.81	26.27	1.5419	1.5373	1.5404	0.0046
PI-7	11.09	26.57	1.5192	1.5287	1.5224	0.0095
PI-8	10.27	33.06	1.5083	1.5016	1.5060	0.0067
PI-ref [g]	9.2	0	–	–	1.6950	0.0780

[a] Film thickness.
[b] Fluorine content.
[c] In-plane refractive index.
[d] Out-of-plane refractive index.
[e] Average refractive index.
[f] Birefringence.
[g] See Ref. [46].

(<60%), respectively. Additionally, the light transmittances at 450 nm of the fluorinated polyimides with high film thickness are not linearly increased by adding of the fluorine loadings in the polyimide backbones. For instance, the 6FDA-based polyimide film with 100 μm thickness (PI-4), having the highest fluorine loadings, exhibited the lowest light transmittance at 450 nm (<55%), demonstrating that the light transmittance of the fluorinated polyimides are not only affected by the fluorine loading but also by the polymer backbone structures (Table 5).

The refractive indices of the fluorinated polyimides measured at the wavelength of 1310 nm using a prism coupler are shown in Table 5. The in-plane (n_{TE}) and out-of-plane (n_{TM}) refractive indices, as well as the average refractive indices (n_{AV}) were measured in the range of 1.5083–1.5641, 1.5016–1.5585 and 1.5060–1.5622, respectively. The n_{AV} values (1.5060–1.5622) of the fluorinated polyimides were much lower than those of the non-fluorinated polyimide such as PMDA–ODA (1.6950) [46] and the reported fluorinated polyimides [43,44], obviously due to the unique fluorine impact contribution. The ratios of in-plane/out-of-plane birefringence (Δn) of the fluorinated polyimide films were ranged of 0.0032 to 0.0095, much lower than that of the polyimide derived from PMDA and ODA (0.0780) [46]. The low birefringence are mainly attributed to the flexible ether linkages and the steric hindered segments in the polymer chains, which resulted in the increase of polymer chain mobility and decrease of polymer chain packing density [47].

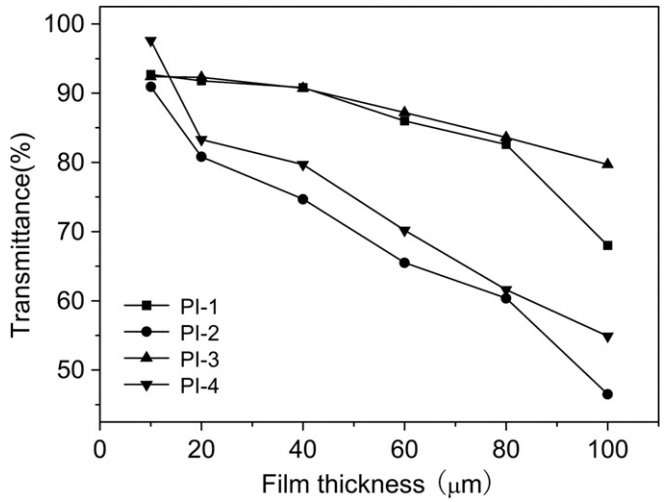

Fig. 9. Plot of the light transmittance at 450 nm *vs* polyimide film thickness.

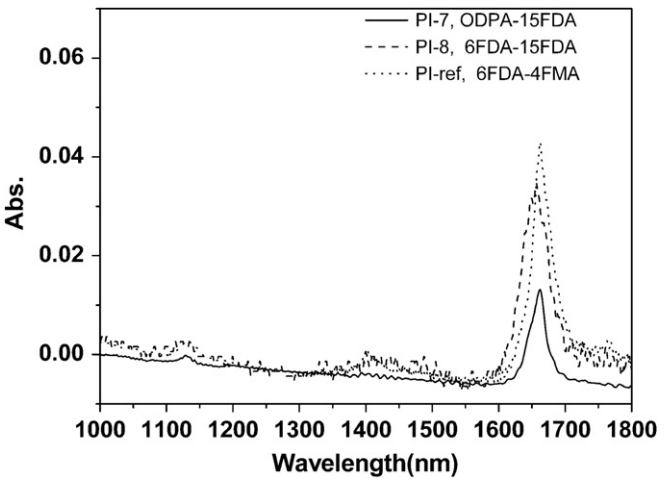

Fig. 10. Near-infrared spectra of representative polyimdes (film thickness: ~140 μm).

Fig. 10 shows the near-infrared absorptions of two representative polyimides (PI-7, PI-8) compared with a reported polyimide [44]. At the key telecommunication wavelengths (1310 and 1550 nm), PI-7 and PI-8 showed very low absorption intensity, which might be attributed to the high fluorine loadings in the polyimide backbones [48]. It is reported that the near-infrared absorptions of polymer materials could be obviously reduced by replacing of the hydrogen atoms in C–H bonds with heavier atoms such as fluorine (F) and chlorine (Cl), or deuterium atom (D) [49,50]. Furthermore, the results here suggest that except for introducing C–F bonds directly, multiple $-CF_3$ groups can also be effective to reduce the absorptions at 1310 and 1550 nm.

4. Conclusions

Multitrifluoromethyl-substituted aromatic diamines were synthesized, which were employed to react with various aromatic dianhydrides by a one-step thermal polycondensation procedure to yield a series of highly fluorinated aromatic polyimides. Experimental results indicated that the aromatic polyimides synthesized showed great solubility both in common low boiling point solvents and in strong polar solvents with inherent viscosities of 0.47–0.69 dL/g. Polyimide films prepared by solution-casting method exhibited good thermal stability with the glass transition temperature (T_g) of 209–239 °C and outstanding mechanical properties with the tensile strengths of 88–111 MPa and tensile modulus of 2.65–3.17 GPa. Dielectric constants of as low as 2.49 and low moisture absorptions (0.17–0.66%) were measured. The fluorinated polyimide films also showed highly optical transparency with transmittance at 450 nm of as high as 97.0% and cutoff wavelength of as low as 298 nm. The refractive indices and birefringence of the polyimide films were measured in the range of 1.5060–1.5622 and 0.0036–0.0095, respectively. Low absorption intensities in near-infrared region, especially at the optocommunication wavelengths (1310 nm and 1550 nm) were also observed in the polyimides.

Acknowledgement

Funding from National Nature Science Foundation of China (NSFC) (No. 50903087) is gratefully acknowledged.

References

[1] Mittal KL, editor. Polyimides: synthesis, characterization and applications, vols. 1 and 2. New York: Plenum; 1984.
[2] Ghosh MK, Mittal KL, editors. Polyimides: fundamentals and applications. New York: Dekker; 1996.
[3] Mittal KL, editor. Polyimides and other high temperature polymers, vol. 1. Utrecht: VSP; 2001.
[4] Mittal KL, editor. Polyimides and other high temperature polymers: synthesis, characterization and applications, vol. 2. Utrecht: VSP; 2003.
[5] Yesodha SK, Sadashiva Pillai CK, Tsutsumi N. Prog Polym Sci 2004;29:45–74.
[6] Maier G. Prog Polym Sci 2001;26:3–65.
[7] Ando S. J Photopolym Sci Tec 2004;17:219–32.
[8] Liaw DJ, Chang FC, Leung MK, Chou MY, Muellen K. Macromolecules 2005;38:4024–9.
[9] Dine-Hart RA, Wright WW. Macromol Chem 1971;143:189–206.
[10] Ando S, Matsuura T, Sasaki S. Polym J 1997;29:69–76.
[11] Hasegawa M, Horie K. Prog Polym Sci 2001;26:259–335.
[12] Seino H, Haba O, Ueda M, Mochizuki A. Polymer 1999;40:551–8.
[13] Morino S, Yamashita T, Horie K, Wada T, Sasabe H. React Funct Polym 2000;44:183–8.
[14] Song GS, Lee JH, Jung SB, Lee YK, Choi HR, Koo JC, et al. Polymer 2007;48:3248–55.
[15] Lin SH, Li FM, Cheng Stephen ZD, Harris FW. Macromolecules 1998;31:2080–6.
[16] Yang CP, Tang SY. J Polym Sci Part A Polym Chem 1999;37:455–64.
[17] Zhou HW, Liu JG, Qian ZG, Zhang SY, Yang SY. J Polym Sci Part A Polym Chem 2001;39:2404–13.
[18] Hergenrother PM, Watson KA, Smith Jr JG, Connell JW, Yokota R. Polymer 2002;43:5077–93.
[19] Leu CM, Chang YT, Wei KH. Chem Mater 2003;15:3721–7.
[20] Yang CP, Hsiao SH, Wu KL. Polymer 2003;44:7067–78.
[21] Xu JW, Chng ML, Chung TS, He CB, Wang R. Polymer 2003;44:4715–21.
[22] Banihashemi A, Abdolmaleki A. Eur Polym J 2004;40:1629–35.
[23] Sasaki T, Moriuchi H, Yano S, Yokota R. Polymer 2005;46:6968–75.
[24] Watanabe Y, Shibasaki Y, Ando S, Ueda M. Polymer 2005;46:5903–8.
[25] Yang CP, Su YY. Polymer 2005;46:5797–807.
[26] Qiu ZM, Wang JH, Zhang QY, Zhang SB, Ding MX, Gao LX. Polymer 2006;47:8444–52.
[27] Wang CY, Li G, Jiang JM. Polymer 2009;50:1709–16.
[28] Lee WF, Lin CH, Hsiao SH, Chung CL. J Polym Sci Part A Polym Chem 2009;47:1756–70.
[29] Liu Y, Zhang YH, Guan SW, Li L, Jiang ZH. Polymer 2008;49:5439–45.
[30] Chung CL, Hsiao SH. Polymer 2008;49:2476–85.
[31] Zhao X, Li YF, Wang XL, Ma T, Yang FC, Shao Y. J Polym Sci Part A Polym Chem 2006;44:6836–46.
[32] Yang CP, Su YY, Wen SJ, Hsiao SH. Polymer 2006;47:7021–33.
[33] Yang CP, Hsiao SH, Hsu MF. J Polym Sci Part A Polym Chem 2002;40:524–34.
[34] Yang CP, Hsiao SH, Chen KH. Polymer 2002;43:5095–104.
[35] Qian ZG, Ge ZY, Li ZX, He MH, Liu JG, Pang ZZ, et al. Polymer 2002;43:6057–63.
[36] Qian ZG, Pang ZZ, Li ZX, He MH, Liu JG, Fan L, et al. J Polym Sci Part A Polym Chem 2002;40:3012–20.
[37] Yang SY, Ge ZY, Yin DX, Liu JG, Li YF, Fan L. J Polym Sci Part A Polym Chem 2004;42:4143–52.
[38] Yin DX, Li YF, Yang HX, Yang SY, Fan L, Liu JG. Polymer 2005;46:3119–27.
[39] Li HS, Liu JG, Wang K, Fan L, Yang SY. Polymer 2006;47:1443–50.
[40] Li HS, Liu JG, Rui JM, Fan L, Yang SY. J Polym Sci Part A Polym Chem 2006;44:2665–74.
[41] Ge ZY, Fan L, Yang SY. Eur Polym J 2008;44:1252–60.
[42] Xie K, Zhang SY, Liu JG, He MH, Yang SY. J Polym Sci Part A Polym Chem 2001;39:2581–90.
[43] Zhao XJ, Liu JG, Rui JM, Fan L, Yang SY. J Appl Polym Sci 2007;103:1442–9.
[44] Zhao XJ, Liu JG, Yang HX, Fan L, Yang SY. Eur Polym J 2008;44:808–20.
[45] Boese D, Lee H, Yoon DY, Swalen JD, Rabolt JF. J Polym Sci Part B Polym Phys 1992;30:1321–7.
[46] Russell TP, Gugger H, Swalen JD. J Polym Sci Polym Phys Ed 1983;21:1745–56.
[47] Badarau C, Wang ZY. Macromolecules 2004;37:147–53.
[48] Groh W. Makromol Chem 1988;189:2861–74.
[49] Kaino T. J Polym Sci Part A Polym Chem 1987;25:37–46.
[50] Yen CT, Chen WC, Liaw DJ, Lu HY. Polymer 2003;44:7079–87.